

TIT/HEP-268/COSMO-47
UTAP/189-94
September 1994

Angular two-point correlation functions for cosmological gamma-ray burst model

SHIHO KOBAYASHI, SHIN SASAKI

Department of Physics, Tokyo Institute of Technology, Oh-okayama, Tokyo 152, Japan.

and

YASUSHI SUTO

Department of Physics, The University of Tokyo, Bunkyo-ku, Tokyo 113, Japan

Submitted to Int. J. Mod. Phys. D

Abstract

We compute the angular two-point correlation functions of the gamma-ray bursts at cosmological distances. Since the gamma-ray burst emission mechanism is not yet established, we simply assume that the gamma-ray burst sources are associated with high-redshift galaxies in some way. Then on the basis of several simple models for the evolution of galaxy spatial correlations, we calculate the amplitude of angular two-point correlation functions on scales appropriate for the Compton Gamma Ray Observatory data. we find that in most cases the predicted correlations are difficult to detect with the current data rate and the angular resolution, but models in which the bursts preferentially occur at relatively low redshift ($z \lesssim 0.5$) predict correlation amplitudes on $\theta \sim 5^\circ$ which will be marginally detectable with the Gamma Ray Observatory data in several years. If future observations detect a signal of angular correlations, it will imply useful information on the correlation of galaxies at high redshifts provided that the gamma-ray bursts are cosmological.

PACS number(s): 95.85.Pw, 98.62.Py, 98.80.Es

1. Introduction

The origin of the gamma-ray bursts (GRBs) remains one of the challenging puzzles in high-energy astrophysics. Although several models to account for the violent energy production have been proposed so far, none of them seems to be successful in explaining various observed features of the GRBs including typical light curves, energy spectra, source distributions, in a consistent and convincing manner¹. Nevertheless the high degree of isotropy in the angular distribution of GRBs observed by the BATSE (Burst and Transient Source Experiment) on the *Gamma Ray Observatory* (GRO) can be interpreted as a strong case for the cosmological origin whatever the emission mechanism is². In particular, a V/V_{\max} test is a very stringent argument in favor of cosmological origin³.

If the GRBs are cosmological, the most natural idea is that the GRB sources are associated with galaxies at redshifts around and up to $z = (1 \sim 2)^{2, 3}$. If this is the case, the angular distribution of the GRBs should trace that of distant galaxies, provided that the GRB event rate be constant in time and insensitive to the host galaxies. Therefore the cosmological model for the GRBs implies that the accumulating number of the GRBs detected by GRO should eventually reveal the underlying angular correlation which is expected for the distant galaxies.

In the present paper, we employ several simple models for the evolution of galaxy correlation functions, and compute the angular two-point correlation functions of the GRBs assuming that the GRB event rate is constant. We find that some models predict correlation amplitudes on $\theta \sim 5^\circ$ which will be marginally detectable with the GRO data in several years. The predicted amplitude would become significantly larger if we assume that the GRBs are preferentially associated with distant rich clusters as preliminarily reported by Cohen, Kolatte and Piran⁴.

The rest of the paper is organized as follows. In §2 our model for the evolution of galaxy correlations and the GRBs is presented. §3 describes the predictions of the angular two-point correlation $w_{GRB}(\theta)$ for the GRBs, and examines the dependence on the several model parameters. Finally §4 discusses the detectability of the correlation, and the implications of the present results.

2. Models

Throughout the present paper, we adopt a simple hypothesis that GRBs are of cosmological origin. To be more specific, we assume that they are associated with distant galaxies and that their event rate is independent of host galaxies, for simplicity. With these assumptions, our present model is basically specified by two quantities; one is the probability of the GRB event per galaxy per unit time, $\phi(z)$, and the other is the spatial two-point correlation function of galaxies, $\xi_{gg}(x, z)$.

Since no specific model for the GRB sources is available which enables to predict the form of $\phi(z)$, we consider two simple cases. Model A assumes that the GRB event rate is constant

from some critical redshift z_c until the present:

$$\phi^A(z(t)) = \begin{cases} \phi_0^A & ; 0 \leq z \leq z_c \\ 0 & ; z_c \leq z \end{cases} . \quad (1)$$

On the other hand, our model B assumes that the GRBs occur for a finite period Δz centered on z_c :

$$\phi^B(z(t)) = \begin{cases} \phi_0^B & ; z_c - \Delta z/2 \leq z \leq z_c + \Delta z/2 \\ 0 & ; \text{otherwise} \end{cases} , \quad (2)$$

where ϕ_0^A and ϕ_0^B are constant and independent of the redshift and host galaxies.

The other important ingredient in computing the angular correlation of the GRBs is $\xi_{gg}(x, z)$. Once dark matter and cosmological parameters are specified, it is fairly straightforward to theoretically predict the two-point correlation functions of *dark matter*. The two-point correlation function of *galaxies*, however, is quite difficult to estimate due to various complicated physical processes involved in galaxy formation. Therefore, we adopt a power-law fit to the present galaxy-galaxy correlation function⁶:

$$\xi_{gg}(x, z = 0) = (x/x_0)^{-\gamma}, \quad x_0 = 5.4h^{-1}\text{Mpc}, \quad \gamma = 1.77, \quad (3)$$

where h is the Hubble constant H_0 in units of 100 km/sec/Mpc. As for the time evolution, we assume that $\xi_{gg}(x, z)$ increases the amplitude independently of x :

$$\xi_{gg}(x, z) = g^2(z, \Omega_0, \lambda_0)\xi_{gg}(x, z = 0) \quad (4)$$

where Ω_0 and λ_0 denote the cosmological density parameter and a dimensionless cosmological constant at present, and $g(z, \Omega_0, \lambda_0)$ is a growth rate of the correlation function. As a growth rate $g(z, \Omega_0, \lambda_0)$, we use either the linear growth rate $D_1(z, \Omega_0, \lambda_0)/D_1(0, \Omega_0, \lambda_0)$, or the power-law parameterization $(1+z)^{-(3+\epsilon-\gamma)/2}$. The parameter ϵ is introduced in order to incorporate the possible nonlinear growth in a very crude manner. If $\epsilon = 0$, the clustering measured in proper coordinates is not changing, and if $\epsilon = -3 + \gamma = -1.23$, that measured in comoving coordinates is not changing. Linear growth rate in the Einstein – de Sitter models corresponds to $\epsilon = \gamma - 1$

3. Angular two-point correlation function of GRBs

3.1 basic equations

We consider the Robertson-Walker metric for the background universe:

$$ds^2 = -dt^2 + a^2(t) \left[\frac{dx^2}{1 - Kx^2} + x^2 d\theta^2 + x^2 \sin^2 \theta d\phi^2 \right], \quad (5)$$

where $a(t)$ is the cosmic scale factor, K is the spatial curvature constant which is related to the cosmological parameters as follows:

$$K = \frac{a_0^2 H_0^2}{c^2} (\Omega_0 + \lambda_0 - 1), \quad (6)$$

where $a_0 \equiv a(t_0)$ is the scale factor at the present time t_0 , and c is the speed of light. The universe is assumed to be dominated by non-relativistic matter. In order to examine the effect of the background universe model, we compute the angular correlation functions of the GRBs, $w_{GRB}(\theta)$, both in open universes without cosmological constant ($\Omega_0 < 0$, $\lambda_0 = 0$) and in spatially flat universes ($\Omega_0 < 0$, $\lambda_0 = 1 - \Omega_0$).

Using the small separation approximation (e.g., §56 in Ref. 5) with the above assumptions, $w_{GRB}(\theta)$ is related to ξ_{gg} as

$$w_{GRB}(\theta) = \frac{\int_0^\infty x^4 dx \frac{\phi^2(z)}{F^2(x)} \int_{-\infty}^\infty du \xi_{gg}(x, z)}{\left[\int_0^\infty dx x^2 \frac{\phi(z)}{F(x)} \right]^2}, \quad (7)$$

where $u \equiv F(x) \sqrt{r^2/a^2 - x^2\theta^2}$, and $F(x) \equiv \sqrt{1 - Kx^2}$. In the above expression, the redshift z should be regarded as a function of the comoving coordinate x through the null geodesic equation. More explicitly, they are related to each other as

$$y \equiv \frac{H_0 a_0 x}{c} = \frac{2[(\Omega_0 - 2)(1 + \Omega_0 z)^{1/2} + 2 - \Omega_0 + \Omega_0 z]}{\Omega_0^2(1 + z)} \quad (8)$$

for $\lambda_0 = 0$, and

$$y = \int_0^z \frac{dz'}{\sqrt{\Omega_0(z' + 1)^3 + 1 - \Omega_0}} \quad (9)$$

for $\lambda_0 = 1 - \Omega_0$.

For the power-law model for $\xi_{gg}(x, z)$ (eq.[4]), the integration over u in eq.(7) can be performed and $w_{GRB}(\theta)$ in this model reduces to⁵

$$w_{GRB}(\theta) = A \theta^{1-\gamma}, \quad (10)$$

$$A \equiv H_\gamma \left(\frac{r_0}{a_0} \right)^\gamma \frac{\int_0^\infty dx \frac{x^{5-\gamma}}{F(x)} \phi^2(z) (1+z)^\gamma g^2(z, \Omega_0, \lambda_0)}{\left[\int_0^\infty dx \frac{x^2 \phi(z)}{F(x)} \right]^2}, \quad (11)$$

where H_γ is a product of Gamma functions; $H_\gamma \equiv \Gamma(1/2)\Gamma((\gamma - 1)/2)/\Gamma(\gamma/2)$. The cosmological model enters through the volume factor F , the relation between x and z (eqs.[8] and [9]), and $g(z, \Omega_0, \lambda_0)$.

3.2 the Einstein – de Sitter model

In the Einstein – de Sitter model with the power-law $\xi_{gg}(x, z)$, the amplitude A of $w_{GRB}(\theta)$ (eq.[11]) can be expressed in terms of the hypergeometric function ${}_2F_1$:

$$A = H_\gamma \left(\frac{H_0 r_0}{c} \right)^\gamma \frac{9}{6 - \gamma} \times \begin{cases} y_c^{-\gamma} \tilde{f}(y_c/2) & ; \text{(model A)} \\ \frac{y_+^{6-\gamma} \tilde{f}(y_+/2) - y_-^{6-\gamma} \tilde{f}(y_-/2)}{(y_+^3 - y_-^3)^2} & ; \text{(model B)} \end{cases}, \quad (12)$$

$$\tilde{f}(y) \equiv {}_2F_1(6 - \gamma, 2\gamma - 2\epsilon - 6, 7 - \gamma; y), \quad (13)$$

$$y_c \equiv 2[1 - (1 + z_c)^{-1/2}], \quad (14)$$

$$y_\pm \equiv 2[1 - (1 + z_c \pm \Delta z/2)^{-1/2}]. \quad (15)$$

When $\Delta z \ll z_c \ll 1$, the above expressions reduce to

$$A \simeq H_\gamma \left(\frac{H_0 r_0}{c} \right)^\gamma \times \begin{cases} \frac{9}{6 - \gamma} z_c^{-\gamma} & ; \text{(model A)} \\ \frac{z_c^{1-\gamma}}{\Delta z} & ; \text{(model B)} \end{cases}. \quad (16)$$

Figure 1 plots the amplitude of w_{GRB} at $\theta = 5^\circ$ as a function of z_c in the Einstein – Sitter model. The angular scale $\theta = 5^\circ$ roughly corresponds to the angular resolution for the GRO. Thus mainly we refer to the amplitude at this scale in the analysis below. The angular correlation $w(5^\circ)$ decreases with z_c since the number of accidental neighbors from the foreground and background increases with z_c and thus the angular correlation is reduced. The difference of evolution of correlation function of galaxies appears at $z_c > 1$. At a given z , the spatial correlation function for smaller ϵ is larger than that for larger ϵ . Thus, the angular correlation function decreases with ϵ , and this effect appears at high redshift. In Figure 2, we show a contour of $w_{GRB}(5^\circ)$ for model B on a $(z_c, \Delta z/z_c)$ plane.

3.3 Open and spatially-flat cosmological models

When the background cosmological model is general or the $\xi_{gg}(x, z)$ is not simply assumed to be a power-law, one has to numerically evaluate the integral of eq.(7). The linear growth rates of fluctuations, D_1 , are explicitly given by

$$D_1 = 1 + \frac{3}{b_1} + \frac{3(1 + b_1)^{1/2}}{b_1^{3/2}} \ln \left[(1 + b_1)^{1/2} - b_1^{1/2} \right], \quad (17)$$

$$b_1 \equiv (\Omega_0^{-1} - 1)a/a_0 \quad (18)$$

for $\lambda_0 = 0$ models, and by

$$D_1 = \sqrt{1 + \frac{2}{b_2^3}} \int_0^{b_2} \left(\frac{b_2'}{2 + b_2'^3} \right) db_2' \simeq \frac{0.2b_2 + 0.044b_2^{1.37}}{1 + 0.328b_2^{1.37}}, \quad (19)$$

$$b_2 \equiv 2^{1/3}(\Omega_0^{-1} - 1)^{1/3} a/a_0 \quad (20)$$

for $\lambda_0 = 1 - \Omega_0$ models. For $\lambda_0 = 1 - \Omega_0$ models, we use an empirical fitting formula (19) in the present computation⁸.

Figures 3a and 3b illustrate $w_{GRB}(5^\circ)$ as a function of Ω_0 for models A and B, respectively (with $z_c = 0.5$, and $\Delta z/z_c = 0.1$). When the growth rate is given independently of the value of Ω_0 (as in our power-law models for g), the angular scale θ corresponds to the smaller physical length in the larger Ω_0 model. Thus the amplitude of w_{GRB} at a given θ becomes larger for larger Ω_0 since it is mainly contributed by the spatial correlation ξ_{gg} on smaller length scales. This is not the case when the growth rate g depends on Ω_0 . Since we normalize the amplitude of ξ_{gg} at the present epoch, lower Ω_0 models, especially $\lambda_0 = 0$ cases, should have higher amplitude of ξ_{gg} in the past (since linear density fluctuations do not grow for $z \lesssim \Omega_0^{-1}$.) This is why the amplitude of w_{GRB} decreases with increasing Ω_0 (for $\lambda_0 = 0$ cases) when we adopt linear growth rate for $g(z, \Omega_0, \lambda_0)$. In any case, the variation of the predicted amplitude of w_{GRB} for different is very small, and at most within a factor of 2.

3.4 CDM spectrum

So far we adopted power-law models (eq.[3]) for the spatial correlations of galaxies. As an example based on fairly specific theoretical models, let us consider the cold dark matter (CDM) models assuming that galaxies trace mass (dark matter). In this case, we adopt $\xi(x, z)_{gg}$ computed from the CDM power spectrum $P(k, z)$ in linear theory:

$$\xi_{gg}(x, z) = \frac{1}{2\pi^2} \int P(k, z) \frac{\sin kx}{kx} k^2 dk. \quad (21)$$

As for $P(k, z)$, we use a fitting formula for the primordial Harrison-Zel'dovich spectrum⁷:

$$P(k, z) = C_0 D_1(z) k \left[\frac{\ln(1 + 2.34q)}{2.34q} \right]^2 \left[1 + 3.89q + (16.1q)^2 + (5.46q)^3 + (6.71q)^4 \right]^{-1/2}, \quad (22)$$

where $q \equiv k/(\Omega_0 h^2 \text{Mpc}^{-1})$, and the amplitude C_0 is fixed so that the top-hat filtered mass fluctuation becomes unity at $r = 8h^{-1} \text{Mpc}$ (see, e.g. Ref.8).

We evaluate $\xi_{gg}(x, z = 0)$ and $w_{GRB}(\theta)$ numerically in the CDM model, which are shown in Figures 4 and 5 for model A in the Einstein-de Sitter model ($\Omega_0 = 1.0$, $\lambda_0 = 0.0$ and $h = 0.5$). The amplitude of $w_{GRB}(\theta)$ for the CDM model rapidly decreases if the angle is larger than the angle spanning the horizon scale at the equality epoch which locates at $z \simeq z_c$. This is because the amplitude of $\xi_{gg}(x, z = 0)$ for the CDM model decreases rapidly outside the horizon scale at the equality epoch. Incidentally this may provide useful information of z_c and Ω_0 , if the angular scale of the zero-point of $w_{GRB}(\theta)$ is detectable¹⁰.

4. Discussion and conclusions

It is important to ask here whether or not the amplitude of $w_{GRB}(\theta)$ predicted in the previous section is detectable. This is checked as follows. The expected number of GRB pairs at

separation θ to $\theta + \delta\theta$ is

$$\langle DD(\theta) \rangle \delta\theta = \frac{N_{GRB}}{2} \frac{N_{GRB}}{4\pi} [1 + w_{GRB}(\theta)] 2\pi\theta\delta\theta, \quad (23)$$

where N_{GRB} is the number of observed GRBs homogeneously surveyed over the 4π steradian. A statistically significant estimate of $w_{GRB}(\theta)$ requires that the number of pairs in excess of random (the second term in RHS of eq.[23]) should be at least larger than the shot noise fluctuation given by

$$\langle \Delta DD(\theta) \rangle \delta\theta = \sqrt{\frac{N_{GRB}}{2} \frac{N_{GRB}}{4\pi}} 2\pi\theta\delta\theta. \quad (24)$$

This implies that given $w_{GRB}(\theta)$, θ , and $\delta\theta$, one needs

$$N_{GRB} \geq 2300 \left(\frac{10^{-2}}{w_{GRB}(\theta)} \right) \sqrt{\frac{5^\circ}{\theta}} \sqrt{\frac{5^\circ}{\delta\theta}}. \quad (25)$$

The lower bound on N_{GRB} for successful detection of $w_{GRB}(5^\circ)$ is listed in the last row in Table 1. Taking into account the BATSE detection rate of GRBs ~ 1 per day⁹, the amplitude of w_{GRB} in most models is rather small for successful detection. Nevertheless it is marginally detectable in some models (for instance, model A with $z_c \leq 0.3$, model B with $z_c = 1.0$, $\Delta z/z_c = 0.1$ and $\epsilon = -3 + \gamma$) with GRBs observed by BATSE in several years.

This difficulty in detecting w_{GRB} is partly ascribed to the low angular resolution of the currently available γ -ray detectors. In fact, it would be much easier to detect w_{GRB} at small angular separations for a given number of sources; $w_{GRB}(\theta) \propto \theta^{1-\gamma}$ for power-law model (see Fig. 4). The correlation of GRBs at 1° is about three times as large as that at 5° , and the necessary number of GRBs reduces factor of 1.4. In this respect, radio, optical and X-ray follow-up observations, if successful, would provide us very valuable information on w_{GRB} .

Recently, Cohen, Kolatte and Piran⁴ reported a possible association of GRBs with rich clusters. As long as neutron stars are involved in GRB events, this association would be difficult to explain. Therefore their report is a serious challenge for the GRB mechanism with neutron stars. On the other hand, if their claim turns out to be real, the amplitude of w_{GRB} would become significantly larger than computed in the previous section since clusters of galaxies are known to be much more strongly clustered than galaxies; depending on the richness of clusters which GRBs are associated with, the amplitude would be enhanced by even an order of magnitude. Then $w_{GRB}(5^\circ)$ would be detectable in a few years for most evolutionary models considered here.

In summary, we employ several simple models for the evolution of galaxy correlation functions, and compute the angular two-point correlation functions of the GRBs assuming that the GRB event rate is constant. On the basis of the plausible evolutionary models for galaxy clustering up to $z \lesssim 1$, the predicted amplitudes of w_{GRB} at 5° scale are generally too small to be detected with the current γ -ray instruments, although some (optimistic) models predict marginally detectable values. Such small amplitudes are mainly due to our simplifying assumption that the GRBs faithfully reflect the clustering at high redshift galaxies. Without

any other convincing theory, we believe that this assumption is most plausible and realistic. Nevertheless the amplitudes of the angular correlation functions may become significantly larger than our predictions either if the GRBs are associated with highly biased species of galaxies (including a possible association of rich clusters) or if the galaxy clustering around $z \lesssim 1$ is much stronger than what standard cosmological models predict. Obviously either case seems rather unrealistic, but cannot be ruled out until specific GRB model is established.

Therefore even if no positive signature of w_{GRB} around 5° scales is detected from future data in several years, this is completely consistent with their cosmological models. In turn, in case that w_{GRB} are detected, the result provides us useful information on the correlation of galaxies at high redshifts provided that the GRBs are cosmological.

One of authors (S.K.) acknowledges the support by the Fellowships of Japan Society for the Promotion of Science for Japanese Junior Scientists. This research was supported in part by the Grants-in-Aid by the Ministry of Education, Science and Culture of Japan (05640312, 06233209).

References

- [1] O.M. Blaes, *ApJS* **92**, 643 (1994).
- [2] B. Paczyński, *Acta Astron.* **41**, 257 (1991).
- [3] S. Mao and B. Paczyński, *ApJL* **288**, L45 (1992).
- [4] E. Cohen, T. Kolatt and T. Piran, preprint (1994).
- [5] P.J.E. Peebles, *The Large Scale Structure of the Universe* (Princeton University Press, Princeton, 1980).
- [6] M. Davis and P.J.E. Peebles, *ApJ* **267**, 465 (1983).
- [7] J.M. Bardeen, J.R. Bond, J.R., N. Kaiser, and A.S. Szalay, *ApJ* **304**, 15 (1986).
- [8] Y. Suto, *Prog. Theor. Phys.* **90**, 1173 (1993).
- [9] C. Kouveliotou, *ApJS* **92**, 637 (1994).
- [10] A. Klypin and G. Rhee *ApJ* **428**, 399 (1994).

Table 1. Summary of $w_{GRB}(5^\circ)$.

| model | z_c | $\Delta z/z_c$ | Ω_0 | λ_0 | ϵ | $w_{GRB}(5^\circ)$ | N_{GRB} |
|-------|-------|----------------|------------|-------------|-------------|----------------------|-----------|
| A | 0.5 | – | 1.0 | 0.0 | 0 | 2.9×10^{-3} | 7900 |
| A | 1.0 | – | 1.0 | 0.0 | 0 | 9.7×10^{-4} | 24000 |
| B | 0.5 | 0.1 | 1.0 | 0.0 | 0 | 1.7×10^{-2} | 1400 |
| B | 1.0 | 0.1 | 1.0 | 0.0 | 0 | 6.2×10^{-3} | 3700 |
| A | 0.5 | – | 1.0 | 0.0 | $-3+\gamma$ | 4.3×10^{-3} | 5300 |
| A | 1.0 | – | 1.0 | 0.0 | $-3+\gamma$ | 1.9×10^{-3} | 12000 |
| B | 0.5 | 0.1 | 1.0 | 0.0 | $-3+\gamma$ | 2.7×10^{-2} | 800 |
| B | 1.0 | 0.1 | 1.0 | 0.0 | $-3+\gamma$ | 1.5×10^{-2} | 1500 |
| A | 0.5 | – | 0.2 | 0.0 | 0 | 2.5×10^{-3} | 9200 |
| A | 1.0 | – | 0.2 | 0.0 | 0 | 7.5×10^{-4} | 31000 |
| B | 0.5 | 0.1 | 0.2 | 0.0 | 0 | 1.3×10^{-2} | 1700 |
| B | 1.0 | 0.1 | 0.2 | 0.0 | 0 | 4.2×10^{-3} | 5500 |
| A | 0.5 | – | 0.2 | 0.0 | $-3+\gamma$ | 3.7×10^{-3} | 6200 |
| A | 1.0 | – | 0.2 | 0.0 | $-3+\gamma$ | 1.5×10^{-3} | 15000 |
| B | 0.5 | 0.1 | 0.2 | 0.0 | $-3+\gamma$ | 2.2×10^{-2} | 1100 |
| B | 1.0 | 0.1 | 0.2 | 0.0 | $-3+\gamma$ | 9.8×10^{-3} | 2300 |
| A | 0.5 | – | 0.2 | 0.8 | 0 | 1.9×10^{-3} | 12000 |
| A | 1.0 | – | 0.2 | 0.8 | 0 | 5.1×10^{-4} | 45000 |
| B | 0.5 | 0.1 | 0.2 | 0.8 | 0 | 9.3×10^{-3} | 2500 |
| B | 1.0 | 0.1 | 0.2 | 0.8 | 0 | 2.6×10^{-3} | 8800 |
| A | 0.5 | – | 0.2 | 0.8 | $-3+\gamma$ | 2.9×10^{-3} | 7900 |
| A | 1.0 | – | 0.2 | 0.8 | $-3+\gamma$ | 1.0×10^{-3} | 23000 |
| B | 0.5 | 0.1 | 0.2 | 0.8 | $-3+\gamma$ | 1.5×10^{-2} | 1500 |
| B | 1.0 | 0.1 | 0.2 | 0.8 | $-3+\gamma$ | 6.2×10^{-3} | 3700 |

Figure captions

Figure 1. The angular two-point correlation functions of GRBs at $\theta = 5^\circ$ as a function of z_c in the Einstein – de Sitter model. The thick solid, dotted and thin solid lines represent results for $\epsilon = 0$, $\epsilon = -3 + \gamma$ and linear growth rate, respectively. (a) model A; (b) model B with $\Delta z/z_c = 0.1$.

Figure 2. The contourlines of $w_{GRB}(5^\circ)$ in the $(z_c, \Delta z/z_c)$ plane for model B (the Einstein – de Sitter model). The thick solid, dotted and thin solid lines represent results for $\epsilon = 0$, $\epsilon = -3 + \gamma$ and linear growth rate, respectively.

Figure 3. The angular correlation $w_{GRB}(5^\circ)$ plotted against Ω_0 . Thick lines indicate results for models without cosmological constant, while thin lines for spatially flat models ($\lambda_0 = 1 - \Omega_0$). Solid, dotted, and dashed lines correspond to $\epsilon = 0$ and $-3 + \gamma$, and linear growth rate, respectively. (a) model A with $z_c = 0.5$, (b) model B with $z_c = 0.5$ and $\Delta z/z_c = 0.1$.

Figure 4. The two-point correlation function of galaxies plotted against separation x (the Einstein-de Sitter model). Solid line corresponds to the CDM model ($\Omega_0 = 1.0$, $\lambda_0 = 0.0$ and $h = 0.5$), while dotted line corresponds to a power-law model.

Figure 5. The angular two-point correlation function of GRBs plotted against angular separation θ . Thick and thin lines indicate results for CDM model and for power-law model. In both cases, we adopt model A for $\phi(z)$ with $z_c = 1.0$ and 0.1 , and linear growth rate in the Einstein-de Sitter model for g .

Kobayashi, Sasaki and Suto
Angular two-point correlation functions
for cosmological gamma-ray burst model
Fig.1

Kobayashi, Sasaki and Suto
Angular two-point correlation functions
for cosmological gamma-ray burst model
Fig.2

Kobayashi, Sasaki and Suto
Angular two-point correlation functions
for cosmological gamma-ray burst model
Fig.3a

Kobayashi, Sasaki and Suto
Angular two-point correlation functions
for cosmological gamma-ray burst model
Fig.3b

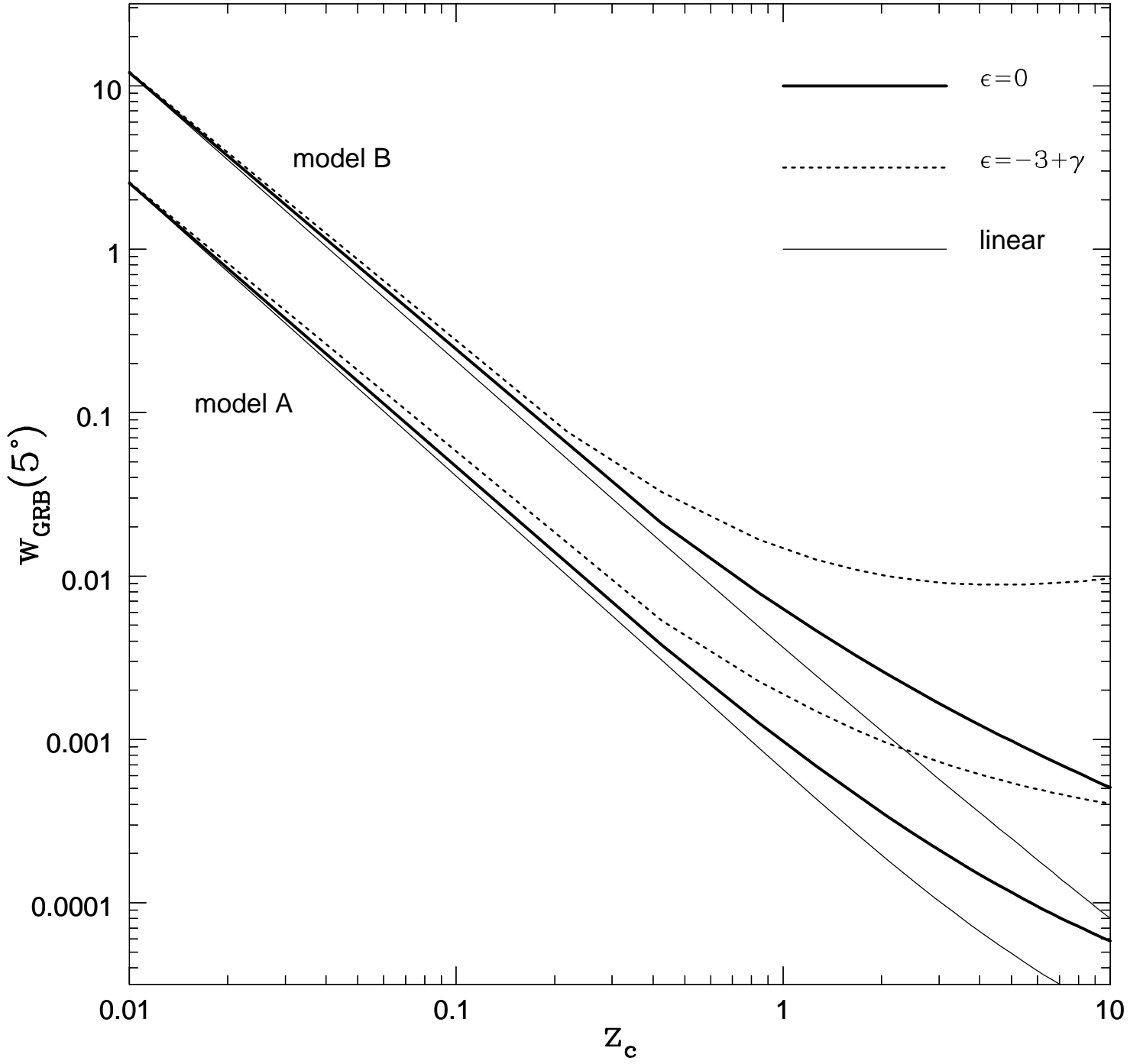
Kobayashi, Sasaki and Suto
Angular two-point correlation functions
for cosmological gamma-ray burst model
Fig.4

Kobayashi, Sasaki and Suto
Angular two-point correlation functions
for cosmological gamma-ray burst model
Fig.5

This figure "fig1-1.png" is available in "png" format from:

<http://arxiv.org/ps/astro-ph/9409043v1>

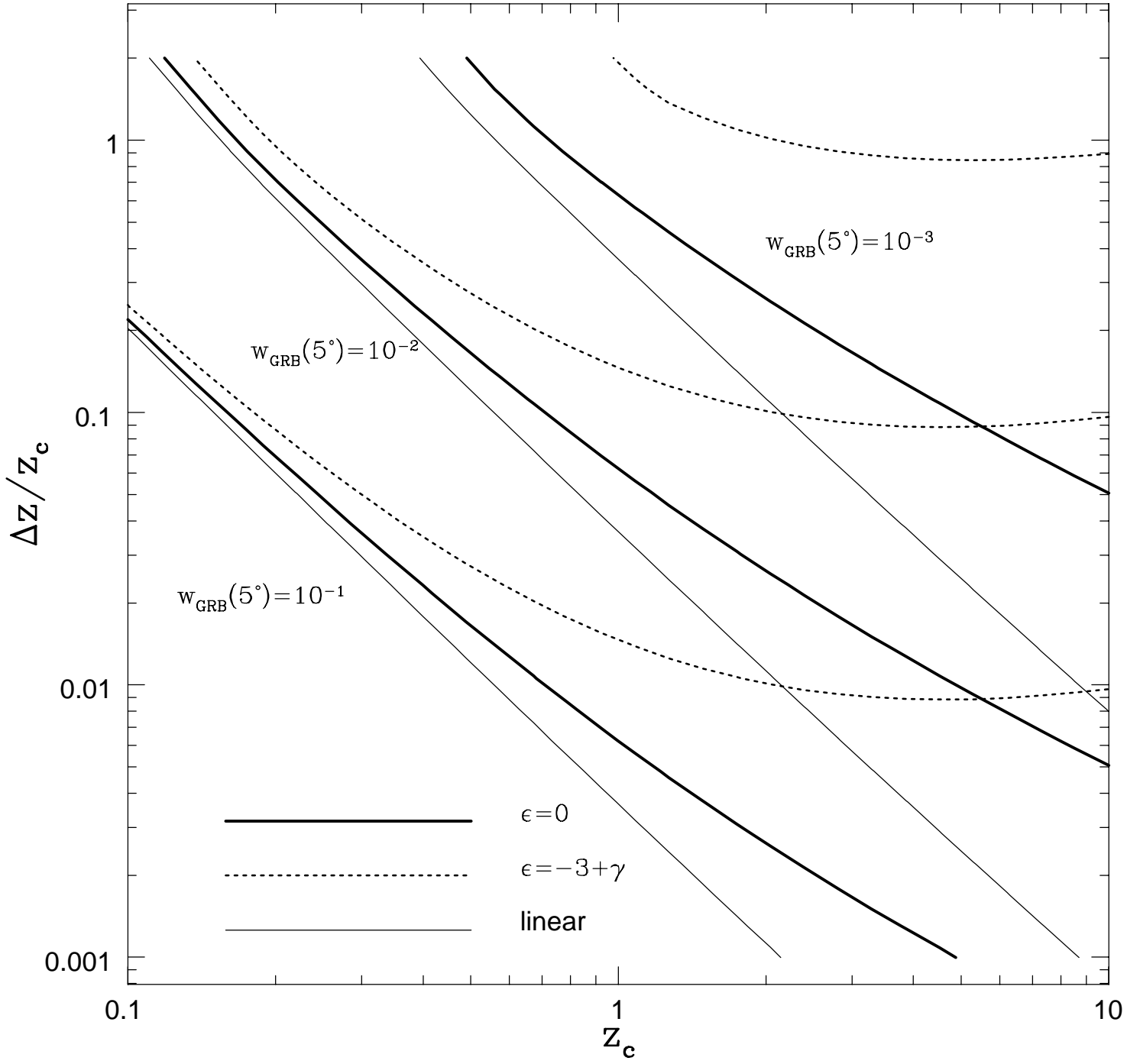
Fig.1



This figure "fig1-2.png" is available in "png" format from:

<http://arxiv.org/ps/astro-ph/9409043v1>

Fig.2



This figure "fig1-3.png" is available in "png" format from:

<http://arxiv.org/ps/astro-ph/9409043v1>

Fig.3a

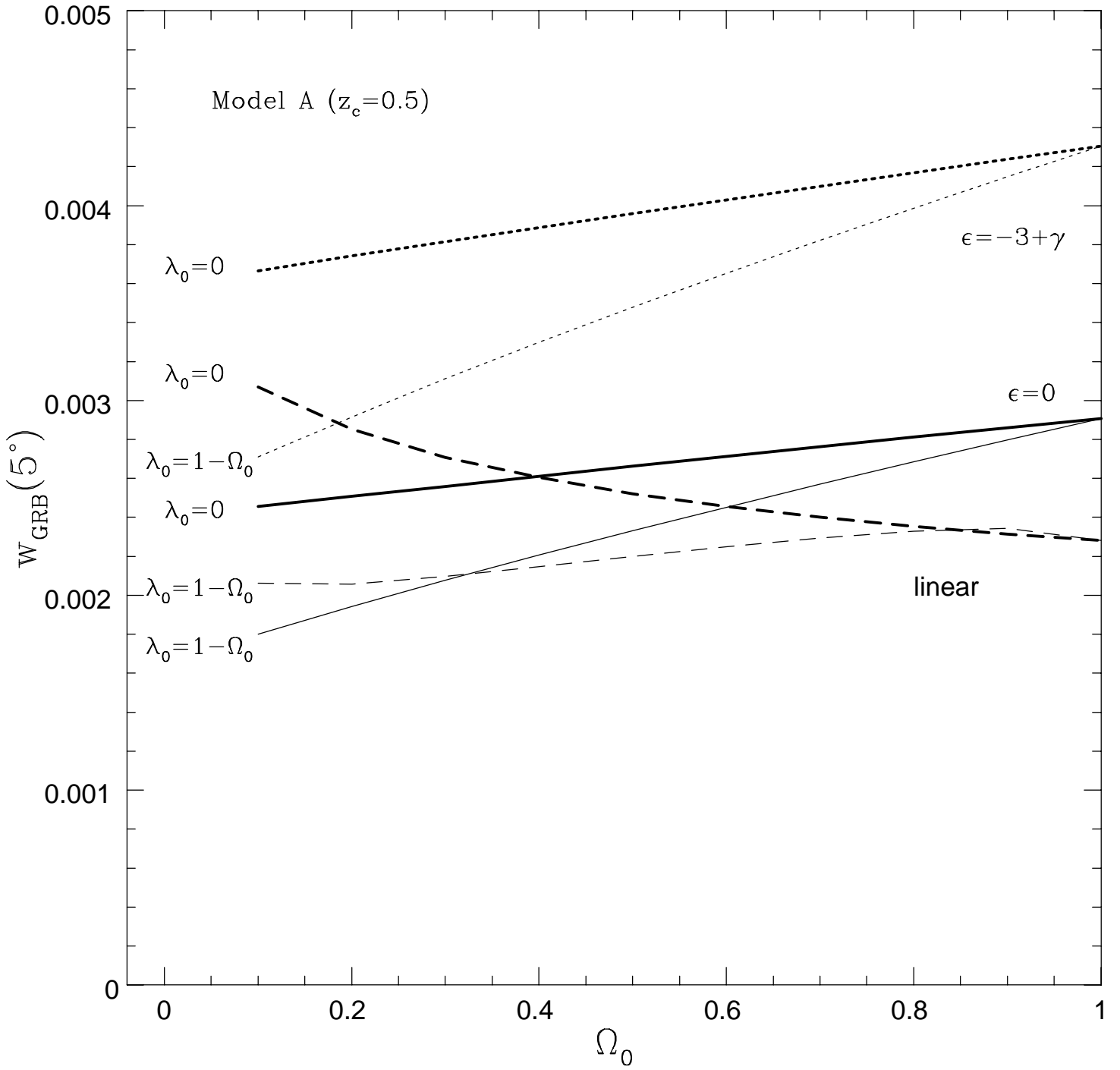
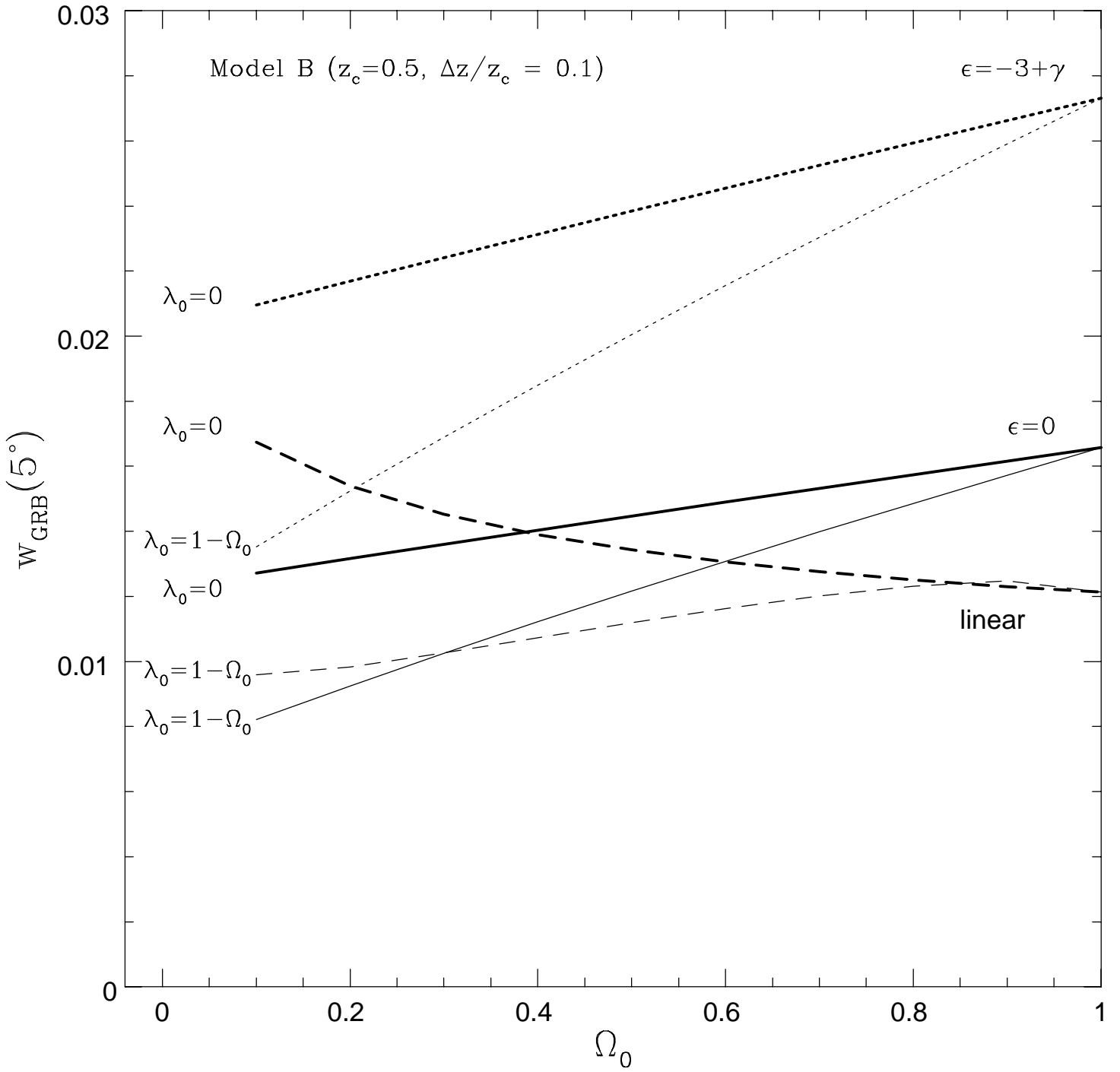


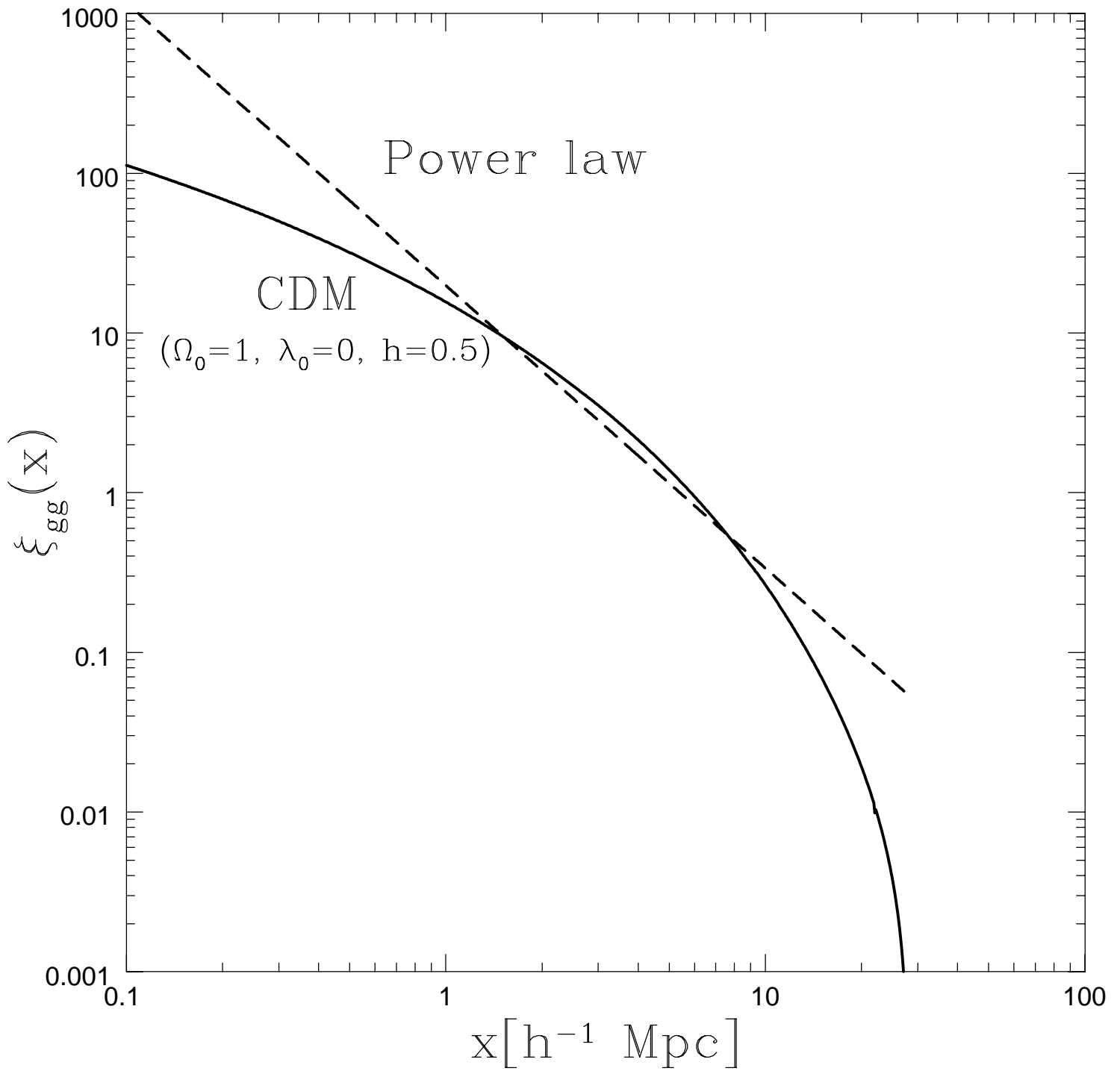
Fig.3b



This figure "fig1-4.png" is available in "png" format from:

<http://arxiv.org/ps/astro-ph/9409043v1>

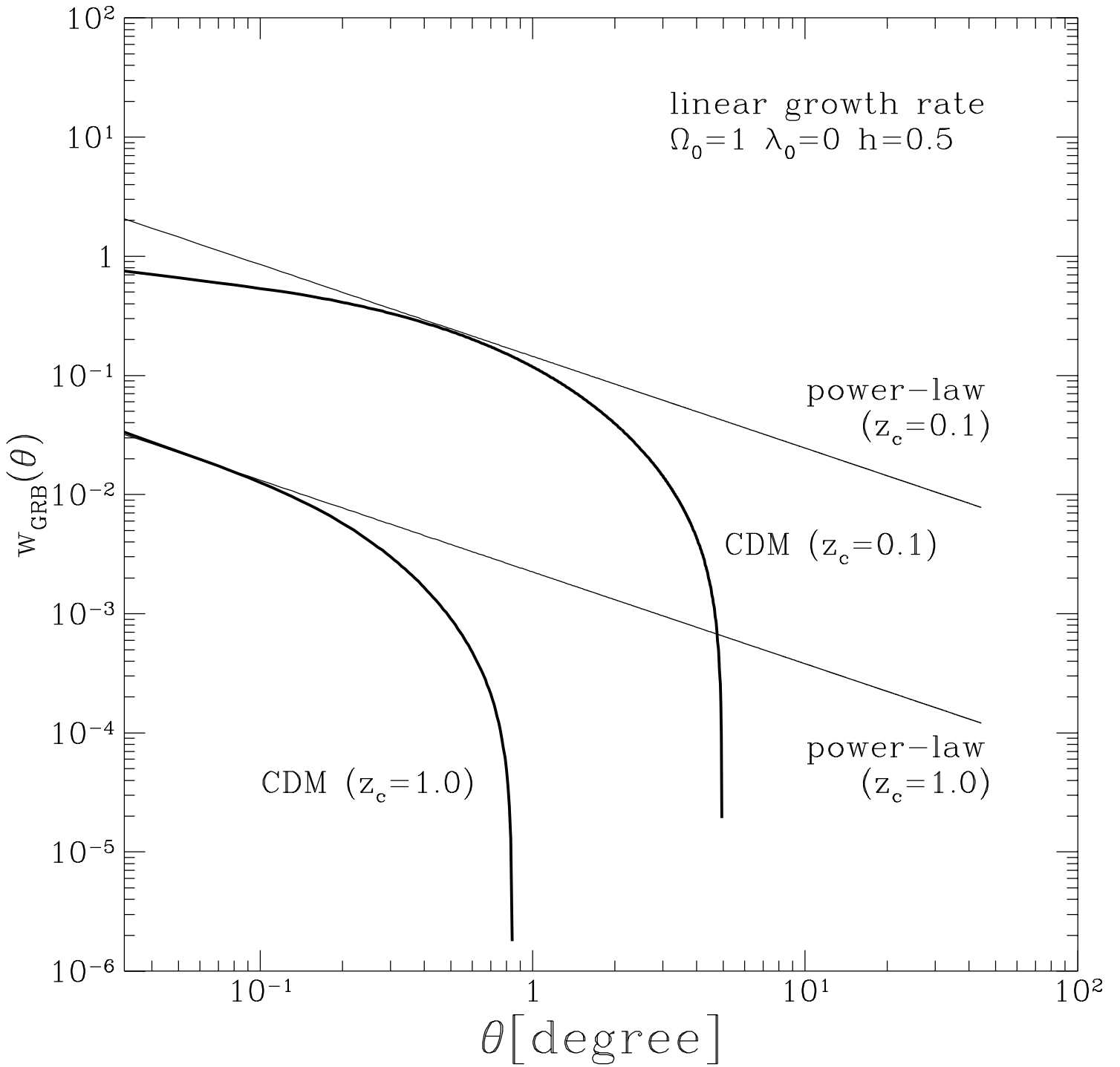
Fig.4



This figure "fig1-5.png" is available in "png" format from:

<http://arxiv.org/ps/astro-ph/9409043v1>

Fig.5



This figure "fig1-6.png" is available in "png" format from:

<http://arxiv.org/ps/astro-ph/9409043v1>